

## Journal Pre-proof

Direct optimisation based model selection and parameter estimation using time-domain data for identifying localised nonlinearities

Sina Safari, Julián M. Londoño Monsalve

PII: S0022-460X(21)00128-0  
DOI: <https://doi.org/10.1016/j.jsv.2021.116056>  
Reference: YJSVI 116056

To appear in: *Journal of Sound and Vibration*

Received date: 28 May 2020  
Revised date: 7 January 2021  
Accepted date: 25 February 2021

Please cite this article as: Sina Safari, Julián M. Londoño Monsalve, Direct optimisation based model selection and parameter estimation using time-domain data for identifying localised nonlinearities, *Journal of Sound and Vibration* (2021), doi: <https://doi.org/10.1016/j.jsv.2021.116056>



This is a PDF file of an article that has undergone enhancements after acceptance, such as the addition of a cover page and metadata, and formatting for readability, but it is not yet the definitive version of record. This version will undergo additional copyediting, typesetting and review before it is published in its final form, but we are providing this version to give early visibility of the article. Please note that, during the production process, errors may be discovered which could affect the content, and all legal disclaimers that apply to the journal pertain.

© 2021 Published by Elsevier Ltd.

# Direct optimisation based model selection and parameter estimation using time-domain data for identifying localised nonlinearities

Sina Safari<sup>a,\*</sup>, Julián M. Londoño Monsalve<sup>a</sup>

<sup>a</sup>College of Engineering, Mathematics and Physical Sciences, University of Exeter, UK

---

## Abstract

A major difficulty when modelling nonlinear structures from experimental vibration data is to determine the type of nonlinear functions that will better predict its dynamic response. In this paper we address this issue by developing a recursive framework in which the characteristics and parameters of nonlinear structures are identified using measured input and output time-domain data. Forward-backward and exhaustive search regression algorithms are exploited based on optimisation techniques to recursively select and quantify the best nonlinear functions from a predefined library of nonlinear terms. **The framework assumes localised nonlinearities for which their location is assumed to be known.** The proposed methodology is demonstrated using numerical and experimental examples of single and multi-degree-of-freedom systems. **The results presented highlight key advantages of the proposed method including: the capability of treating multi-degree of freedom nonlinear systems holding different types of localised nonlinearities, and the capability of selecting nonlinear terms with a light computational effort and with limited number of time samples.**

**Keywords:** Nonlinear System Identification, Data Driven Model, Nonlinearity Characterisation, Nonlinear Structures, **Modal coupling**, Nonlinear Optimisation Algorithm.

---

## 1. Introduction

There has been much recent interest in developing methods for delivering mathematical models capable of predicting the behaviour of structures with nonlinearities. This is mainly due to the fact that industrial applications demand more efficient and lightweight structures which results in structural designs that are more prone to nonlinear effects. Experimental modal analysis has been widely developed and implemented throughout the academia and industry to identify systems with linearity and superposition assumptions [1]. Nonetheless, the lack of knowledge about the mechanism of nonlinearity in structures while in service has encouraged the development of nonlinear system identification (NSI) methods to identify nonlinear models using vibration test data.

Linear structural systems are commonly identified from vibration data using conventional Frequency response functions (FRFs). However nonlinear structures cannot be identified based on such FRF data since the superposition principle does not apply to nonlinear systems and as the averaging process required for estimating FRFs would likely lead to the inability to capture detailed nonlinear behaviours such as sudden jumps in vibration regime and bifurcations. To deal with nonlinear systems, numerous methods have been developed recently focusing on detection, localisation, characterisation and quantification of nonlinearities in structural systems, many of which have been reviewed in [2]. Detection of nonlinearities can be achieved by simple techniques such as observation of distorted peaks of a FRF or recognition of jumps in time history responses [2]. However the localisation, characterization and quantification techniques applied to nonlinear system identification are still open research topics [3]. It is preferable to have a parsimonious model <sup>1</sup>

---

\*Corresponding author

Email addresses: [ss1072@exeter.ac.uk](mailto:ss1072@exeter.ac.uk) (Sina Safari), [J.Londono-Monsalve@exeter.ac.uk](mailto:J.Londono-Monsalve@exeter.ac.uk) (Julián M. Londoño Monsalve)

<sup>1</sup>The simplest model with great explanatory predictive power that explain data with a minimum number of parameters.

20 **capable of estimating dynamics of system accurately.** Finding the location of nonlinearity is often facilitated by engineering knowledge and can often be narrowed down to a small number of possibilities, typically joints especially for the common engineering structures [4].

In this paper, we will focus on data-driven methods to characterize nonlinear structural dynamics that, in an effort to minimise loss of information, use directly time-domain data. The data used for the identification 25 are normally forced response data or measured resonance decay data. Approaches that use forced response data include among others restoring force surface method [5, 6], reverse path approaches [7, 8], subspace-based techniques [9, 10] and NARMAX [11]. Alternatively, Londoño et al. [12, 13] used resonance decay data to generate backbone curves as a useful tool providing valuable information about system dynamics. **Backbone curves have been also employed for identification of the parameters of nonlinear structures [14–** 30 **16].** In general, backbone curve measurements require emulating undamped and unforced conditions and therefore the experimental extraction of backbone curves remains a challenging topic that has been tackled using control-based continuation [17, 18] and phase-locked-loop techniques [19]. These techniques rely on satisfying phase quadrature criterion which takes place when the single-point harmonic forcing and the displacement at the forcing location are in quadrature, i.e., the phase is locked at an angle equal to  $\pi/2$ . 35 It has been reported by Volvert and Kerschen [20] that the fundamental, superharmonic and subharmonic resonances of nonlinear mechanical systems may exhibit phase lags that are not necessarily equal to  $\pi/2$ . Besides, appropriate forcing to satisfy this criteria was found particularly critical for complex MDOF systems featuring close modes [18, 21].

It is essential to ensure that any mathematical model selected in the context of NSI process is physically 40 meaningful and capable of predicting the performance of structures in operational and extreme loading conditions. In most common NSI methods an ansatz is made as an educated guess for the type of nonlinearity prior to parameter estimation [10, 22, 23]; on the other hand, in methods that do not require an ansatz, the delivered model are not typically parsimonious [24]. For example, the polynomial nonlinear state space (PNLSS) method [24] uses best linear approximation (BLA) to initialise nonlinear system identification in 45 the state space. The high number of the polynomial parameters generated for nonlinear model in the PNLSS method cause the selected model to be not parsimonious. Decoupling methods have also been introduced recently to address this issue [25], however, the number of parameters to be estimated still remains high.

Since selecting a nonlinear model (a candidate), has significant importance and is not yet clearly solved, in this study we proposed a model selection method for nonlinear engineering structures. There are some 50 existing algorithms for model selection. Forward, backward and exhaustive search methods have been developed for nonlinear model selection problems [11, 26, 27]. The methods have been applied for the linear-in-parameters nonlinear models which can be solved using classical least squares-type approaches. However, dealing with nonlinear models that are not linear-in-parameters still have not been completely addressed when it comes to nonlinear model selection for engineering structures. More recently, Ben Abdesslem et al. 55 [28] explored variants of approximate Bayesian computation for model selection and parameter estimation. Their approach requires high computational effort due to the fact that the numerical structural model needs to be run in each iteration to estimate the true parameters based on prior distribution of the parameters. They also search in a predefined library of nonlinear models but do not consider the combination of models in the library which might be the solution for the problem. Taghipour et al. [29] proposed an optimisation-based 60 framework for model selection based on experimental data from stepped sine results. They examined different models comparing the experimental and simulated stepped sine results. Therefore, the framework involves a high computational cost to generate stepped sine data. Reviewing the above-mentioned literatures, it is essential to develop an efficient data-driven model selection framework in time-domain to include nonlinear-in-parameter functions allowing to deliver parsimonious model with light computational effort.

65 In this paper, an optimisation-based data-driven framework is proposed for automated model selection and parameter estimation of proportionally damped structures with localized nonlinearities to overcome the necessity of assuming the type of nonlinearity. The method assumes that the structure behaves linearly at the low levels of vibration and that the location of the nonlinear elements are known. **Unlike the methods reviewed above [28, 29] which require stepped sine tests or running a finite element model in each iteration,** in the method proposed here, the measured inputs: forces and outputs: accelerations, velocities, and 70 displacements are transformed into modal space and directly substituted into the equations of motions so

that a nonlinear model can be fitted using nonlinear regression. Therefore it does not require the solution of the differential equations of motion. Forward-backward and exhaustive search regression approaches are considered in the framework to deliver a parsimonious model and the algorithms select the dominant nonlinear terms from a comprehensive predefined library which includes linear- and nonlinear-in-parameters nonlinear functions. The proposed methodology is initially examined using various numerical examples, and is validated experimentally using a test rig that consists a bolted structure which displays nonlinear behavior. The primary scope is to use time-domain data to identify the nonlinearity form and its parameters for structures with single nonlinear element. The rest of this paper is structured as follow. Section 2 introduces the methodology proposed in this work. Simulated SDOF systems with nonlinear elements are used in Section 3 to explore the features of algorithms applied for model selection and parameter estimation. The procedure is then validated using experimental data in Section 5. In Section 4 applicability of proposed method is demonstrated for Multi-degree-of-freedom (MDOF) systems. The main conclusions are discussed in Section 6.

## 2. The proposed methodology

In this section a methodology for nonlinear system identification of engineering structures including non-linearity characterization and parameter estimation is discussed. We consider a nonlinear system represented by the following equation of motion in physical space:

$$\mathbf{M}\ddot{\mathbf{q}} + \mathbf{C}\dot{\mathbf{q}} + \mathbf{K}\mathbf{q} + \sum_{i=1}^r \rho_i^T f_{nl}(\rho_i, \mathbf{q}) = \mathbf{F} \quad (1)$$

where  $\ddot{\mathbf{q}}$ ,  $\dot{\mathbf{q}}$  and  $\mathbf{q}$  are respectively the acceleration, velocity and displacement  $m \times n$  matrices, where  $m$  is numbers of degrees of freedom and  $n$  is number of time-domain points;  $\mathbf{M}$ ,  $\mathbf{C}$  and  $\mathbf{K}$  are the  $m \times m$  matrices of mass, damping and stiffness,  $\mathbf{F}$  is the force matrix and  $\rho$  is a location vector of the  $r$  nonlinear elements. The function  $f_{nl}$  represents generic nonlinear stiffness force.

The equation of motion can be transformed into linear modal space as in the Eq. (2) using the matrix of linear mode shapes  $\Phi$ . Thus, system dynamics can be expressed in terms of the linear modal coordinates  $u(t)$ .

$$\mathbf{M}_s \ddot{\mathbf{u}} + \mathbf{C}_s \dot{\mathbf{u}} + \mathbf{K}_s \mathbf{u} + \sum_{i=1}^r \Phi^T \rho_i^T f_{nl}(\rho_i, \Phi \mathbf{u}) = \Phi^T \mathbf{F} \quad (2)$$

where  $\mathbf{M}_s = \Phi^T \mathbf{M} \Phi$ ,  $\mathbf{C}_s = \Phi^T \mathbf{C} \Phi$  and  $\mathbf{K}_s = \Phi^T \mathbf{K} \Phi$  are the diagonal modal matrices for mass, damping and stiffness. Diagonal modal matrices indicate decoupling of the equations of motions in the linear part, however coupling among linear modes remain and are due to the presence nonlinear terms in the summation in Eq. (2). This facilitates data manipulation for MDOF systems and reduce the dimension of identification problem which is discussed in Section 4 in more details. For the purpose of nonlinear model identification (i.e. selecting  $f_{nl}$ ), we assumed that the characteristics of underlying linear system i.e. natural frequencies, damping ratios and mode shapes are known and validated experimentally using one of the standard available methods e.g. Polymax [30].

In synopsis, the proposed methodology begins with conducting forced vibration test and then processing the acquired response time-series data. Afterwards, optimisation-based model selection and parameter estimation algorithms used for nonlinear model identification. More detailed description is discussed in the following subsections.

### 2.1. Forced vibration and data processing

Transient responses contains information about all of the underlying fundamental features of a dynamical system, including those properties that are susceptible to change as a function of the vibration amplitude. Therefore, in this study, we are interested in transient response records from the initial part of the system response under harmonic excitation (sine or sweep-sine) and also free vibration response record when setting the system free after achieving a desired response nearby a resonance. Harmonic excitation is used as it

can excite the structure at specific frequencies that are more likely to activate certain nonlinear effects (e.g., opening and closing a joint). It is important to note that the excitation level should satisfy the level of expected performance during the lifetime of the structure. It is due to the fact that the identified model will be accurate over the amplitude region where data is available, but outside it (i.e. where data are not available), there would be no means to assess the reliability of the model. In particular, it is expected that the large displacement response acquired nearby a resonance condition of a nonlinear system would provide more useful information about the nonlinear dynamics of the structure.

The methodology discussed in this paper requires the availability of the following time-domain data: acceleration, velocity and displacement response records and also the applied excitation force. Notice that in case of a numerical studies, all the information could be made available from the numerical solver directly. On the other hand, displacement and velocity response data can be obtained from experimentally measured acceleration data using numerical integration [12, 31, 32], Kalman filtering [33] or wavelet transform [34]. In this work, acceleration response is integrated numerically to calculate velocity and displacement.

Three different approaches are considered by recasting Eq. (2) to show the applicability of the identification method in different levels of information available from structural system. The first approach (Approach I) considers the case when modal mass ( $\mathbf{M}_s$ ), damping ( $\mathbf{C}_s$ ) and linear stiffness ( $\mathbf{K}_s$ ) coefficients in the Eq. (2) are known and only nonlinear forces are unknown. Linear damping and stiffness are also considered to be unknown along the nonlinear part in the second approach (Approach II). Finally, all of the parameters in the Eq. (2) are considered to be unknown and requiring to be identified in the Approach III. The approaches are formularised in Eqs. (3) where the terms in bold and underlined are considered unknown to be found using the proposed method as described in the following section.

$$(I) : \sum_{i=1}^r \Phi^T \rho_i^T \underline{\mathbf{f}}_{nl}(\rho_i \Phi \mathbf{u}) = \Phi^T \mathbf{F} - (\mathbf{M}_s \ddot{\mathbf{u}} + \mathbf{C}_s \dot{\mathbf{u}} + \mathbf{K}_s \mathbf{u}) \quad (3a)$$

$$(II) : \underline{\mathbf{C}}_s \dot{\mathbf{u}} + \underline{\mathbf{K}}_s \mathbf{u} + \sum_{i=1}^r \Phi^T \rho_i^T \underline{\mathbf{f}}_{nl}(\rho_i \Phi \mathbf{u}) = \Phi^T \mathbf{F} - \mathbf{M}_s \ddot{\mathbf{u}} \quad (3b)$$

$$(III) : \underline{\mathbf{M}}_s \ddot{\mathbf{u}} + \underline{\mathbf{C}}_s \dot{\mathbf{u}} + \underline{\mathbf{K}}_s \mathbf{u} + \sum_{i=1}^r \Phi^T \rho_i^T \underline{\mathbf{f}}_{nl}(\rho_i \Phi \mathbf{u}) = \Phi^T \mathbf{F} \quad (3c)$$

## 2.2. Optimisation-based nonlinear model identification

The aim is to identify reliable mathematical models for the stiffness nonlinearities included in the structural system. To this end, the optimization routine is set up to minimise the mean square error ( $MSE$ ) given by Eq. (4) as the cost function that measures the discrepancy between observed and predicted data:

$$\begin{aligned} \text{Minimize : } MSE &= \frac{1}{n} \sum_{i=1}^n (y_{mm_i}^* - y_{mm_i})^2 \\ \text{Subject to : } &\frac{1}{nc} \sum_{j=1}^{nc} \frac{1}{n} \sum_{i=1}^n (y_{cm(j)_i}^* - y_{cm(j)_i})^2 < \varepsilon_c \end{aligned} \quad (4)$$

where  $n$  is the size of the time series data and  $y^*$  and  $y$  are the observed and predicted data which are equal to the right hand side and left hand side of the Eqs. (3) respectively. Subscripts  $mm$  and  $cm$  denote the main and constraint modes and  $nc$  denotes the number of constraint modes. The difference between the main and constraint modes will be explained later in Section 4. Also,  $\varepsilon_c$  is the tolerance of nonlinear inequality constraint which indicates how accurate the estimated model should satisfy the responses of constraint modes.

The optimisation routine is implemented based on different approaches presented in Eqs. (3). The existing parameters of the underlying linear system are assumed to be true and are directly substituted into the equation of motion in Eqs. (3) when considering the approach (I), and the parameter estimation of

135 nonlinear model is subsequently done. To consider cases where the linear parameters are inaccurate, in the approaches (II) and (III) above, the parameters of linear model are estimated in parallel with the parameters of nonlinear model.

For parameter estimation, the optimisation problem defined in Eq. (4) is solved using a gradient-based interior point algorithm. This algorithm, which is available in the `fmincon` function of MATLAB [35], is suitable for parameter estimation of nonlinear-in-parameter models. Besides, scatter search (SS) method [36], which is available in the `GlobalSearch` function of MATLAB [35], is used to run the aforementioned gradient-based optimisation algorithm multiple times to reach a global optimum solution. It starts searching from different scattered initial points in the neighbourhood of user-defined initial point.

145 It is important to express the nonlinear optimisation problem in terms of scaled parameters. This will facilitate the convergence of gradient-based optimisation algorithm. For this purpose, parameters in Eqs. (3) are scaled linearly based on the observed maximum force and responses. For example, maximum displacement is used to scale dead space or gap distance parameter in the dead-zone nonlinear model so that the scaled search space is bounded to  $[0,1]$ . This example is studied in Section 3.

150 In addition, for better chances of reaching a global minimum, the initial values and bounds for the parameters need to be carefully selected. The existing parameters of the underlying linear system from linear modal testing i.e. damping ratios and natural frequencies of the system are used to initialise the respective variables of the linear parameters when considering approaches (II) and (III). Lower upper bounds are set for the linear parameters considering reliable linear modal identification. In this way small inaccuracies in primarily identified linear parameters can be compensated for. For the parameters of nonlinear models, the algorithm considers initial values and bounds assigned by the user in the scaled space as explained for dead-zone nonlinear model above.

160 Once the optimisation problem is defined, nonlinear model selection is carried out using two independent optimisation-based algorithms: the forward regression nonlinear optimization (FRNLO) + backward regression nonlinear optimization (BRNLO) and the exhaustive search nonlinear optimization (ESNLO) algorithms. Both algorithms use a predefined and comprehensive library of nonlinear models typically encountered in common engineering applications as the one shown in Table 1. The main concept behind the algorithms are discussed below.

FRNLO algorithm works out the nonlinear model of a system as follows:

- 165 • Step 1: Add one nonlinear term at a time from the library of nonlinear terms to the structural model in Eqs. (3) (when FRNLO starts, it includes the linear part only) and calculate the cost function using Eq. (4).
- Step 2: Try a different nonlinear term from the library of nonlinear terms and calculate the respective cost function using Eq. (4).
- 170 • Step 3: Once all nonlinear terms present in the library have been independently examined, select and add the nonlinear term with the minimum cost function value to the structural model and eliminate that term from the library of nonlinear terms.
- Step 4: Check the stopping criteria based on Eqs. (4,5), if not satisfied go to Step 1 and iterate.
- Step 5: If stopping criteria is satisfied then deliver the nonlinear structural model.

175 It should be mentioned that the estimated parameters of current iteration are fed to FRNLO algorithm in order to initialise the next iteration. FRNLO delivers the nonlinear model with an initial set of terms, however, some nonlinear terms initially recognized by the algorithm might have negligible contribution to the system dynamics, which only become evident when other terms are added. Therefore, we introduce BRNLO to eliminate terms with negligible contribution and to provide a parsimonious model. BRNLO algorithm works as follows:

- 180 • Step 1: Receive the nonlinear structural model and its parameters delivered by FRNLO

- Step 2: Eliminate one nonlinear term from the model at a time and evaluate cost function using Eq. (4) for each combination of remained terms.
- Step 3: Once all models examined after each independent elimination, select and store the nonlinear structural model with the minimum cost.
- 185 • Step 4: Check the stopping criteria based on Eqs. (4,5), if not satisfied go to Step 2 and iterate.
- Step 5: If stopping criteria is satisfied then deliver the nonlinear structural model.

As an alternative, we also consider the ESNLO algorithm which consists of the following steps:

- Step 1: generate all the possible combinations of the candidate nonlinear terms available in the library and categorize them for complexity into groups based on their number of parameters.
- 190 • Step 2: calculate cost function using Eq. (4) for all combinations in category  $s$ .
- Step 3: select the combination with minimum cost in category  $s$ .
- Step 4: Check the stopping criteria based on Eqs. (4,5), if not satisfied go to Step 2 and iterate for  $s=s+1$ .
- Step 5: If stopping criteria is satisfied then deliver the nonlinear structural model.

195 The selected model will be the least complex (smallest number of nonlinear terms) and more accurate model to describe the nonlinear behaviour of the structure.

The steps of the nonlinear system identification method implemented in this paper are also illustrated in Fig. 1. As it can be seen there, once the nonlinear model is selected and parameter estimation is completed, the fitted model goes through validation process.

200 Primarily,  $MSE$  is enforced as stopping criteria for model selection when its value drops lower than user-assigned threshold  $\varepsilon_1$ . Secondly, when the change of two consecutive  $MSE$  values is less than  $\varepsilon_2$  as shown in Eq. (5), the algorithm stops and delivers the nonlinear model. Notice that the later criterion will be determinant in cases when by adding more nonlinear terms, the model prediction accuracy does not improve significantly, and so, the extra complexity is not worth it; in such cases the extra term will be rejected.

$$\frac{\Delta MSE^{(s)}}{\Delta s} < \varepsilon_2 \quad (5)$$

Once system response records are available and the goal of identification is set based on the approaches defined in Eqs. (3), the model selection and parameter estimation method proposed in this work can be initiated.

### 210 3. Application to nonlinear SDOF systems

In this section a series of SDOF systems with stiffness nonlinearity (Fig. 2) are used to illustrate the applicability of the procedure presented above. The load excitation and acceleration response can be measured experimentally or obtained from numerical solver and then velocity and displacement are derived from acceleration using numerical integration [31].

215 Eq. (1) can be rewritten for the case of a nonlinear SDOF system as presented in Eq. (6). A number of stiffness nonlinearities typically encountered in common engineering applications will be examined. In the following examples, the nonlinear model library assumed polynomials up to 7-th order in this study. Two nonlinear models are also included in the library representing non-smooth nonlinearities: the step function and also dead-zone using the forms given in [37] and presented in Table 1.

$$M\ddot{\mathbf{q}} + C\dot{\mathbf{q}} + K\mathbf{q} + f_{nl}(\mathbf{q}) = \mathbf{F} \quad (6)$$

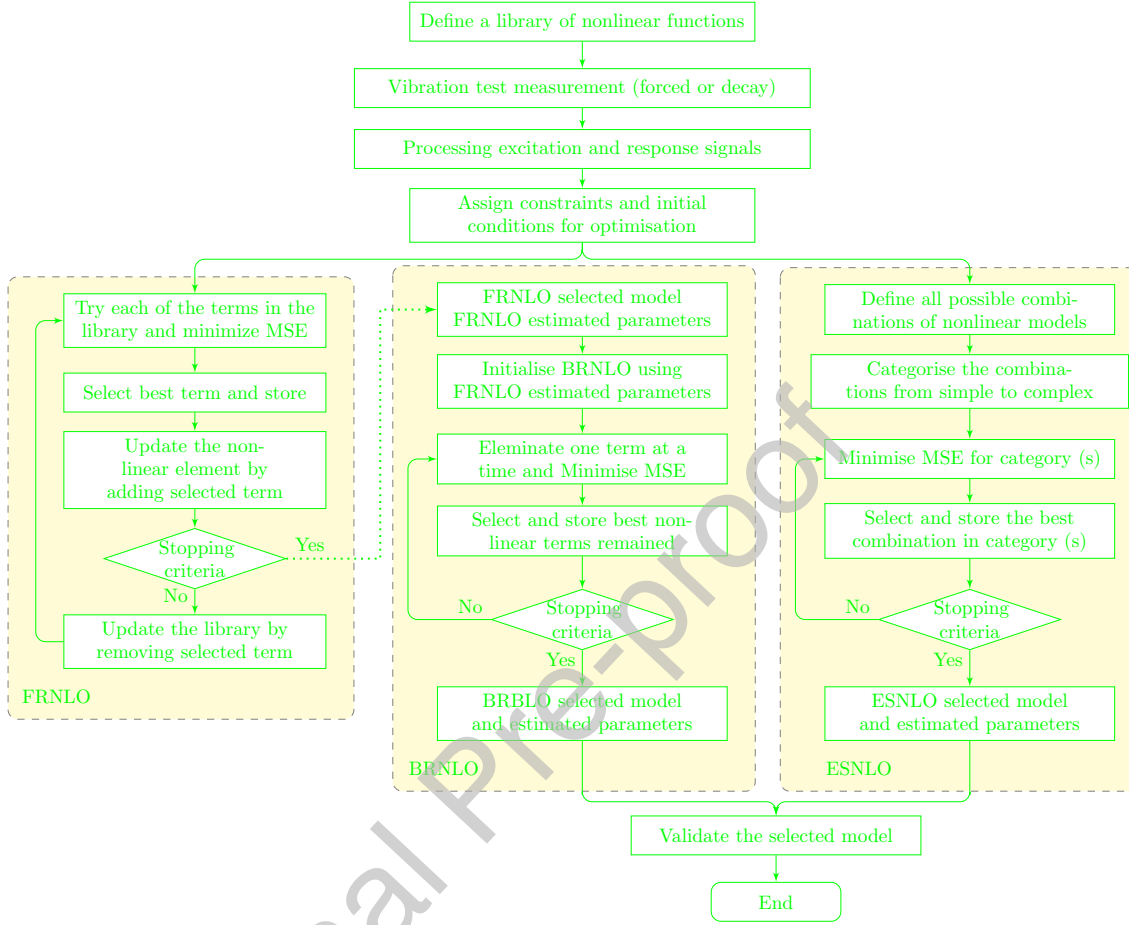


Figure 1: Flowchart of the proposed nonlinear system identification framework.

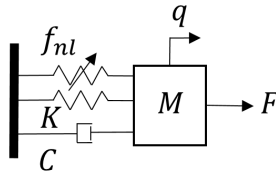


Figure 2: Single degree of freedom system with stiffness nonlinearity.

220 In Table 1,  $F_f$  is the step force,  $K_f$  is the hardening coefficient,  $K_d$  is the stiffness after contact,  $\theta_{r1} = q - \frac{d}{2}$ ,  $\theta_{r2} = q + \frac{d}{2}$ ,  $U(\theta) \cong \frac{1}{2}[\tanh(\sigma_g \theta) + 1]$ , and  $d$  is the backlash or dead space. We note that the constant value  $\sigma_g = 10^7$  is used to define the smoothness of change between the two regimes in the non-smooth functions.

225 Table 2 summarises the type of nonlinearities and the numerical values used in each of the case studies considered below. In addition, the parameters of the underlying linear system named mass, damping ratio and stiffness are assumed to be:  $M = 0.6874$  kg;  $C = 1.35$  N.sec/m and  $K = 3.3 \times 10^4$  N/m ( $f_n = 34.73$  Hz,  $\zeta = 0.0045$ ). A numerical integrator based on Runge-Kutta methods was used to solve the nonlinear



Table 1: Nonlinearities considered in the example SDOF systems.

No.	Nonlinear term $f_{nl}(q)$	No.	Nonlinear term $f_{nl}(q)$
1	$ q q$	7	$\text{sign}(q)\sqrt{ q }$
2	$q^3$	8	$q\sqrt{ q }$
3	$ q q^3$	9	$ q q\sqrt{ q }$
4	$q^5$	10	$q^3\sqrt{ q }$
5	$ q q^5$	11	$F_f \left( \frac{2}{(1+e^{(-\sigma q^q)})} - 1 \right) + K_f q$
6	$q^7$	12	$K_d (\theta_{r2} + [\theta_{r1} U (\theta_{r1}) - \theta_{r2} U (\theta_{r2})])$

differential equation of motion. A transient response of the structure when it is vibrated using a harmonic excitation  $F = F_0 \sin(\omega t)$  is computed and used for nonlinear identification of SDOF examples presented here. The amplitude of harmonic excitation is  $F_0 = 5\text{N}$  and  $\omega$  equals to the natural frequency of the structure.

Table 2: Parameters assigned for nonlinearities in the SDOF system example.

Case	Polynomial			$F_f(\text{N})$	Step	Dead Zone	
	$K_2(\text{N/m}^2)$	$K_3(\text{N/m}^3)$	$K_5(\text{N/m}^5)$			$d(\text{mm})$	$K_d(\text{N/m})$
1	-	$1.05 \times 10^9$	-	-	-	-	-
2	$-9.05 \times 10^5$	$1.05 \times 10^9$	-	-	-	-	-
3	$-9.05 \times 10^5$	$1.05 \times 10^9$	$3.1 \times 10^{13}$	-	-	-	-
4	-	-	-	3	100	-	-
5	-	$1.05 \times 10^9$	-	3	100	-	-
6	-	-	-	-	-	4	$2.7 \times 10^5$

The results will be discussed based on the three above mentioned approaches in Eqs. (3). Moreover, the performance of the proposed nonlinear identification methods: FRNLO, BRNLO and ESNLO are evaluated and compared considering the different approaches. In order to validate the results, the backbone curves estimated from the fitted model are compared with the backbone curves generated for true system using nonlinear resonance decay method (NLRDM) [12]. Further, the stepped sine sweep response of the nonlinear models estimated using the proposed method is shown on top of the backbone curves.

**Case 1: cubic stiffness.** The response shown in Fig. 3 was generated numerically from Eq. (6) using ODE45 in MATLAB for the SDOF system Case 1 in Table 2. Variation in amplitude and presence of higher harmonics can be observed in the internal linear and nonlinear forces presented in Fig. 3(b). The duration of numerical integrating is 3 second with sampling frequency  $F_s = 100f_n$ .

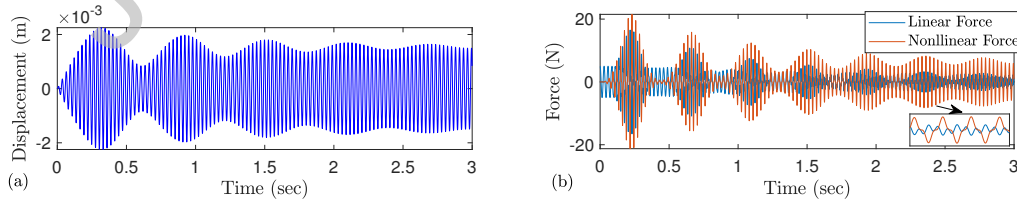


Figure 3: Response of SDOF structure when cubic nonlinearity is considered (a) Displacement (b) Internal forces.

Once the data is generated, the FRNLO algorithm was applied to infer the nonlinear model and estimated its parameters. Both of the stopping criteria were set as  $\varepsilon_1 = \varepsilon_2 = 10^{-6}$ . The tolerance of nonlinear inequality constraint in the Eqs. (4) is also set to  $\varepsilon_c = 10^{-6}$ . The algorithm converges in one iteration and

245 the cubic nonlinear model is selected with  $MSE = 1.833 \times 10^{-18}$ . The trivial value of  $MSE$  for one model suggests that there is no need to initiate the other algorithms, (i.e. BRNLO and ESNLO) however, after running BRNLO, it is also delivers the same model selected by FRNLO. Table 3 reports the identification results error based on the three approaches presented above in Eqs. (3).

250 It can be seen that accurate estimation is achieved and as the level of complexity (estimating both linear and nonlinear part) increases the estimation error shows a slight increase, however, the level of error is within an acceptable level. Fig. 4 compares the identified nonlinear force-displacement and backbone curve results for the SDOF system with cubic nonlinearity. Results show good match between true and estimated force-displacement response and also the estimated backbone curve and generated one using the NLRDM [12]. Finally, they are superimposed onto several synthetic stepped-sine sweep responses for different levels of excitation ( $\mathbf{F}_0 = [0.0125, 0.25, 0.5, 1]N$ ).

Table 3: Identification results for SDOF system case 1: cubic stiffness using FRNLO algorithm.

System parameters		Identification results error (%)		
		approach I	approach II	approach III
M (kg)	0.687	-	-	$9.2 \times 10^{-3}$
C (N.s/m)	1.35	-	$1.6 \times 10^{-14}$	$9.2 \times 10^{-3}$
K (N/m)	$3.27 \times 10^4$	-	$2.2 \times 10^{-14}$	$9.2 \times 10^{-3}$
$K_3(N/m^3)$	$1.05 \times 10^9$	$2.3 \times 10^{-3}$	$1.08 \times 10^{-2}$	$1.3 \times 10^{-2}$

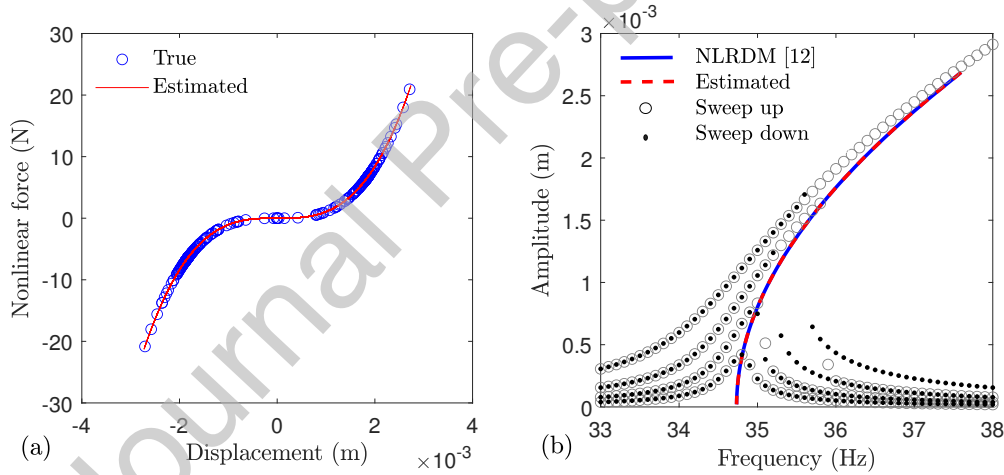


Figure 4: Identification of SDOF with cubic stiffness using the FRNLO algorithm (a) Nonlinear force-displacement response (b) Backbone curves generated from estimated and true system based on [12] overlaying on the stepped-sine simulation responses of true system.

**Case 2: Quadratic and cubic stiffness.** The second case corresponds to a SDOF system that includes a quadratic and cubic stiffness nonlinearities. As before, a transient response of 3 sec duration under harmonic loading is used for identification purpose. The progression of models selection using FRNLO, BRNLO and ESNLO methods is shown in the Fig. 5 in terms of  $MSE$  values and difference between two successive  $MSE$  values, where, the stopping criteria was set as  $\varepsilon_1 = \varepsilon_2 = 10^{-6}$ . The horizontal axis shows the number of nonlinear models selected from library with their models indicated in the caption respectively. Initially, it can be seen that the FRNLO selects four polynomial terms as best fit to the data, following that, BRNLO cross out the two terms with negligible contribution. It is observed from Fig. 5a that  $\Delta MSE^{(s)}/\Delta s$  increases when adding fourth term from the library. The reason is that the  $MSE$  value is highly decreased

265 by adding the fourth term with respect to the previous MSE values and therefore the rate of change of MSE ( $\Delta MSE^{(s)}/\Delta s$ ) in this step is higher than the previous one. For BRBLO, in Fig. 5b, it can be seen that after removing 2 terms, the MSE remains below  $\epsilon_1$ , but when third nonlinear term is removed, the MSE increases, and therefore only 2 terms are removed.

270 Furthermore, ESNLO algorithm follows a straightforward path and identifies the best and simplest combination of nonlinear function to describe the dynamic behaviour of the structure.

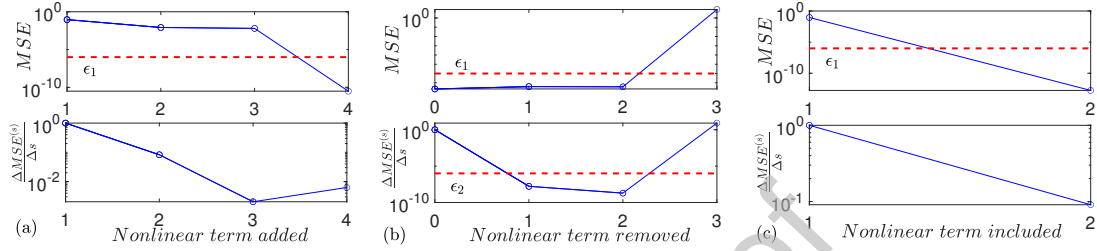


Figure 5: Nonlinear model selection for case 2 based on (a) FRNLO (selected models:  $[|q|q^3, |q|q^5, |q|q, q^3]$ ) (b) BRNLO (selected models:  $[|q|q, q^3]$ ) and (c) exhaustive search (selected models:  $[|q|q, q^3]$ ) algorithms.

The identification results error is reported in Table 4 for nonlinear system with quadric and cubic stiffness nonlinearity. All three approaches presented in Eqs. (3) are examined here. It should be noted that in case of approach II and III, linear parameters from linear modal testing are also used to constrain the optimisation algorithm and provide the initial condition to start the optimisation with. Fig. 6 presents the identification results in terms of nonlinear force-displacement and backbone curves. These results show good agreement between the estimated and true system response. The stepped-sine sweep responses of the identified system with different levels of excitation ( $\mathbf{F}_0 = [0.05, 0.25, 0.5, 1]N$ ) illustrates that the identifies model follows the dynamic behaviour of the structure acceptably.

Table 4: Identification results for SDOF system case 2: quadratic and cubic stiffness using FRNLO+BRNLO algorithm.

System parameters		Identification results error (%)		
		approach I	approach II	approach III
M (kg)	0.687	-	-	$3.4 \times 10^{-3}$
C (N.s/m)	1.35	-	$1.6 \times 10^{-14}$	$3.4 \times 10^{-3}$
K (N/m)	$3.27 \times 10^4$	-	$2.2 \times 10^{-14}$	$3.4 \times 10^{-3}$
$K_2(N/m^2)$	$-9.05 \times 10^5$	$1.1 \times 10^{-4}$	$4 \times 10^{-2}$	$1.5 \times 10^{-2}$
$K_3(N/m^3)$	$1.05 \times 10^9$	$2.4 \times 10^{-3}$	$6.8 \times 10^{-3}$	$4.6 \times 10^{-3}$

280 **Case 3: Quadratic, cubic and Quintic stiffness.** The performance of the proposed identification algorithms for model selection is now investigated by considering a SDOF system with quadratic, cubic and quintic stiffness nonlinearity. As before we assume that the input excitation force is applied to the structure at the system natural frequency in order to generate high amplitude response.

285 The convergence of three proposed algorithm in selecting the best nonlinear model is illustrated in Fig. 7. As it can be seen four nonlinear polynomial term is selected based on FRNLO algorithm with the final MSE value of  $8 \times 10^{-11}$ . Although  $|q|q^3$  is selected as the initial match from FRNLO, the BRNLO algorithm is capable of identifying that the term interfered with the true contributing models as the MSE value decreased to  $7.5 \times 10^{-12}$  by eliminating  $|q|q^3$ . The identification results of ESNLO algorithm are reported in Table 5 and considers the three approaches presented above in Eqs. (3). Again the estimation error in all of the cases is considerably low.

290 Fig. 8a compares the nonlinear force-displacement estimated from the fitted model and from the true model. The results show good agreement even though there are three nonlinearities combined together.

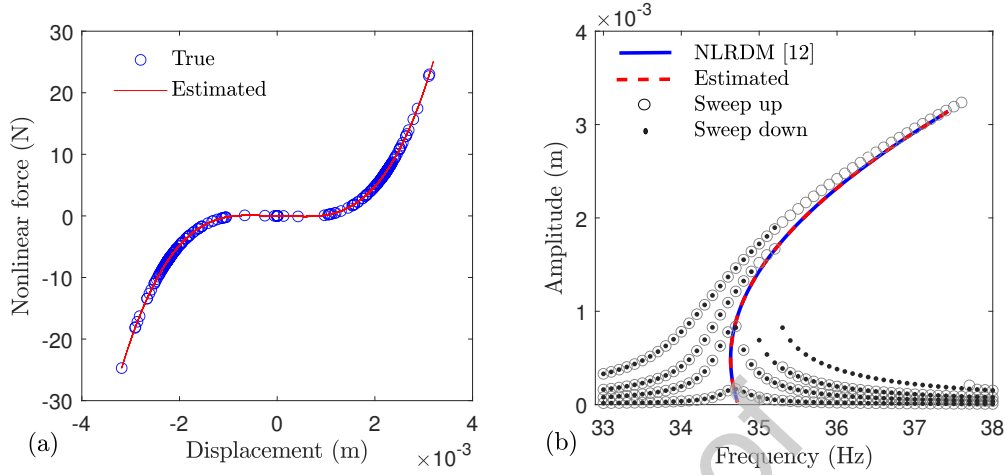


Figure 6: Identification of SDOF with Quadratic+cubic stiffness using the FRNLO+BRNLO algorithms (a) Nonlinear force-displacement response (b) Backbone curves generated from estimated and true system based on [12] overlaying on the stepped-sine simulation responses of true system.

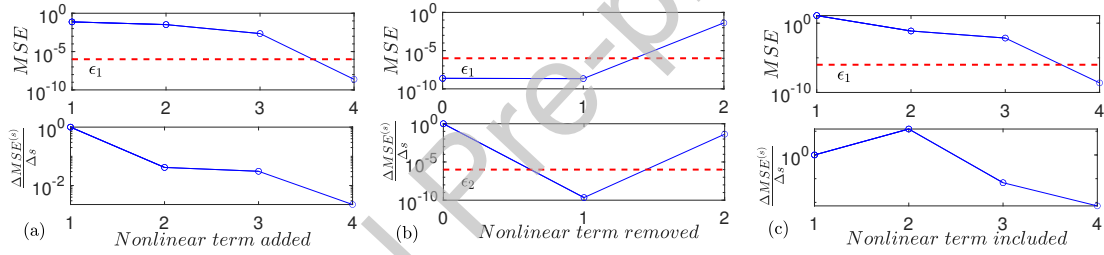


Figure 7: Nonlinear model selection for case 3 based on (a) FRNLO (selected models:  $[|q|q^3, |q|q^5, |q|q, q^3]$ ) (b) BRNLO (selected models:  $[|q|q, q^3]$ ) and (c) ESNLO (selected models:  $[|q|q, q^3]$ ) algorithms.

Table 5: Identification results for SDOF system case 3: Quadratic, cubic and Quintic stiffness using FRNLO+BRNLO algorithm.

System parameters		Identification results error (%)		
		approach I	approach II	approach III
$M$ (kg)	0.687	-	-	$1.5 \times 10^{-3}$
$C$ (N.s/m)	1.35	-	$1.6 \times 10^{-14}$	$1.5 \times 10^{-3}$
$K$ (N/m)	$3.27 \times 10^4$	-	$2.2 \times 10^{-14}$	$1.5 \times 10^{-3}$
$K_2$ (N/m <sup>2</sup> )	$-9.05 \times 10^5$	$1.8 \times 10^{-4}$	$8.3 \times 10^{-2}$	$5.2 \times 10^{-2}$
$K_3$ (N/m <sup>3</sup> )	$1.05 \times 10^9$	$1.2 \times 10^{-3}$	$6 \times 10^{-3}$	$4 \times 10^{-3}$
$K_5$ (N/m <sup>5</sup> )	$1.05 \times 10^9$	$1.6 \times 10^{-3}$	$4 \times 10^{-4}$	$1.3 \times 10^{-2}$

From Fig. 8b, the backbone curve produced based on the identification method in this paper shows a clear match with the backbone curve using NLRDM [12]. For the purpose of validation, the stepped-sine sweep responses of the identified system with different levels of excitation ( $\mathbf{F}_0 = [0.05, 0.25, 0.5, 1, 2]$ N) presented which indicates a successful identification. This example displays different behaviour at low and high amplitude vibration levels and shown that the proposed data-driven method is able to deal with complex and smooth nonlinearities. In terms of computational time, in this example, FRNLO algorithm proceeds in 20 sec, BRNLO in 7.5 sec and ESNLO in 10 sec. It can be seen that the FRNLO+BRNLO results in higher

computational time to accomplish the desired identification result in comparison with ESNLO.

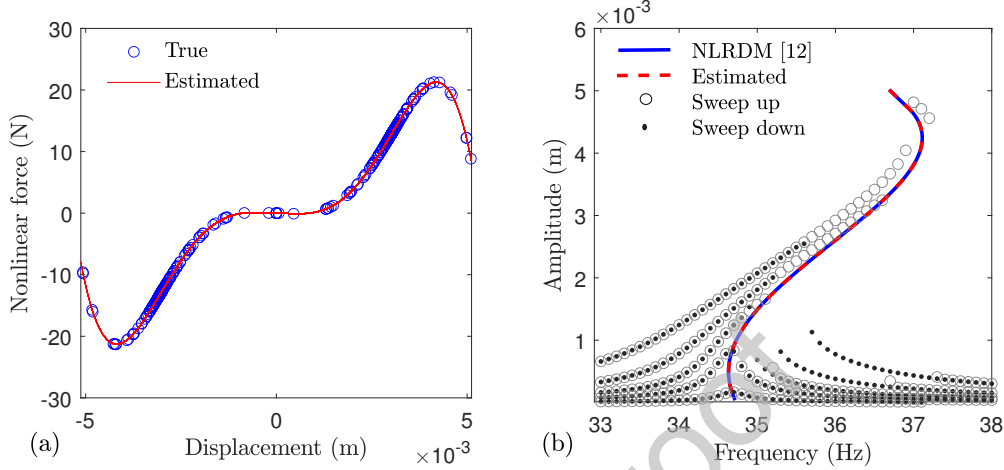


Figure 8: Identification of SDOF with Quadratic+cubic+Quintic stiffness using the ESNLO algorithm (a) Nonlinear force-displacement response (b) Backbone curves generated from estimated and true system based on [12] overlaying on the stepped-sine simulation responses of true system.

300 **Case 4 and 5: Step and cubic stiffness.** To demonstrate the application of developed method to identify nonlinear structures with non-smooth nonlinearities, step function with linear stiffness and the combination of step with cubic stiffness nonlinearity are now investigated. Step function can be used to model locking connection that after released have linear or nonlinear stiffness. Approach III is used to fully identify the dynamic parameters of nonlinear structure for this example. Accurate model selection is achieved using the proposed method in this study. Fig. 9a shows the results for case 4, where the backbone curve estimated using the model fitted by ESNLO algorithm is compared with the true backbone curve identified using NLRDM [12]. Similar result have been seen for FRNLO+BRNLO algorithm which indicates that if proper nonlinear models included in the library the identified model will be selected with negligible error. The FRNLO+BRNLO algorithm results is not reported here for brevity. The identified nonlinear force-displacement results based on ESNLO also shows a good agreement with true simulation results. The stepped-sine sweep responses of the identified system for  $F_0 = [2.8, 5]$ N levels of excitation are overlaid on the backbone curves which show a good agreement. For low excitation level  $F_0 = 2.8$ N and low frequency band, it can be observed that the amplitude of the stepped-sine sweep responses is very small (near zero) which is due to the fact that the system is not vibrating at the resonance condition. Moreover, results for case 5 are presented in Fig. 9b, where a successful estimation of a nonlinear model is achieved. Parameter estimation results for the two cases are reported in Table 6 showing a accurate model prediction.

Table 6: Parameter estimation results for Step nonlinearity.

	Nonlinearity Type				
	Step + Linear stiffness		Step + Cubic stiffness		
	$F_f(N)$	$K_f(N/m)$	$F_f(N)$	$K_f(N/m)$	$K_3(N/m^3)$
Estimation	3	100	3	100	$1.05 \times 10^9$
Error (%)	$2.76 \times 10^{-6}$	$1.64 \times 10^{-5}$	$7.17e \times 10^{-6}$	$4.76 \times 10^{-4}$	$1 \times 10^{-3}$

**Case 6: Dead zone (Backlash).** Non-smooth nature of the nonlinearity can be seen also in the engineering structures like gear backlash nonlinearity [37]. Backlash or dead zone nonlinearity also considered

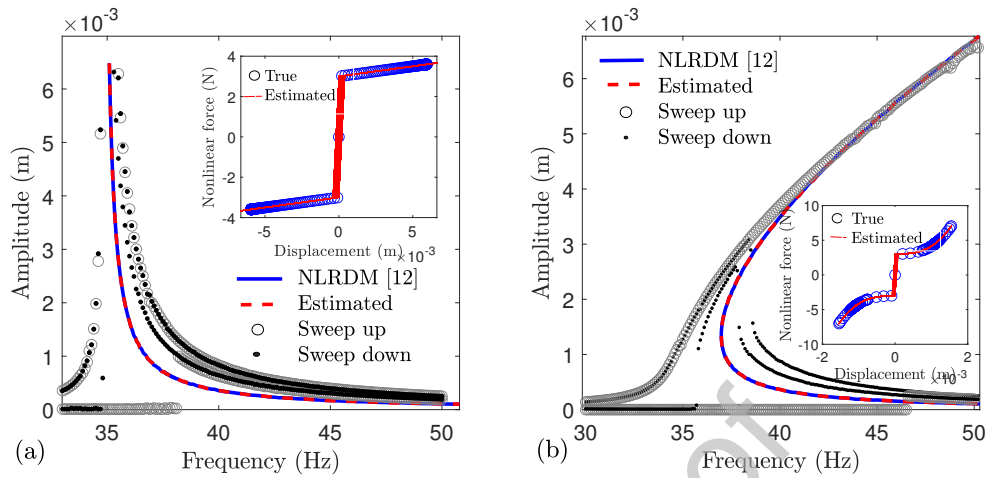


Figure 9: Force-displacement and backbone curves overlaying on the stepped-sine simulation responses ( $\mathbf{F}_0 = [2.8, 5]N$ ) of true system with nonsmooth nonlinearities using the FRNLO+BRNLO algorithms (a) Step + Linear stiffness (b) Step + Cubic stiffness nonlinearities.

in this study using the nonlinear function No. 12 in Table 1. As before, the simulation data are generated for 3 second under harmonic excitation described in Section 3 using the values assigned for Dead zone nonlinearity from Table 2. Again, approach III is used to fully identify the dynamic parameters of nonlinear structure. Fig. 10 shows the backbone curve prediction based on ESNLO algorithm. It can be seen that if the nonlinear function is included in the library of nonlinear terms, the model selection and parameter estimation is successful and can provide accurate prediction of nonlinear dynamics of structure. The stepped-sine sweep responses of the identified system with different levels of excitation ( $\mathbf{F}_0 = [0.25, 0.5, 1, 2]N$ ) are also presented.

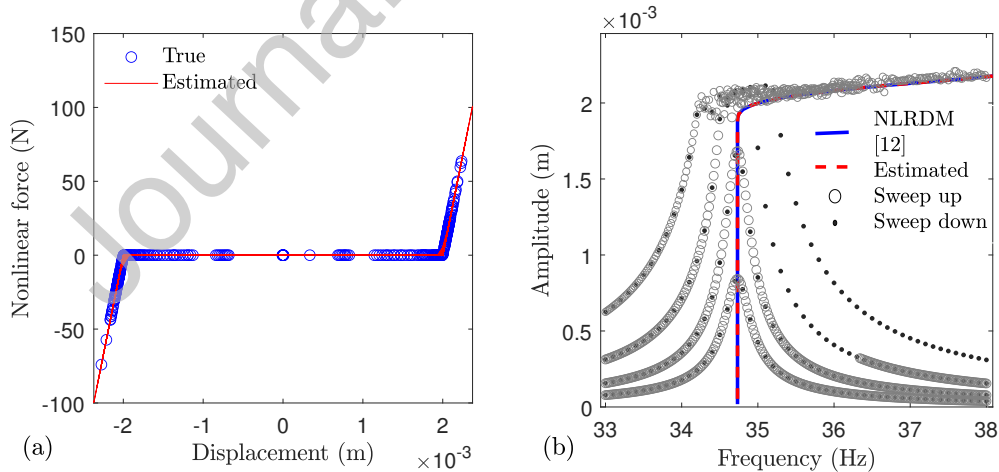


Figure 10: Results for system with Dead zone (Backlash) nonlinearity using the ESNLO algorithm (a) Nonlinear force-displacement response (b) Backbone curves generated for estimated and true system based on [12] overlaying on the stepped-sine simulation responses of true system.

### 3.1. Discussion and sensitivity analysis

In this section we consider some issues that can affect the robustness of the proposed method in the case of practical application. The effects of obtaining velocity and displacement from acceleration measurement, noise in the measured responses and the comprehensiveness in the library of nonlinear terms are first evaluated. The effects of generating velocity and displacement data from measured acceleration on the model selection and parameter estimation are discussed using Case 2 in Table 2 (quadratic+cubic) and considering approach I to identify the nonlinear model. The accelerations were numerically integrated, and the resulting velocity were passed through a first order high-pass Butterworth filter with a cutoff frequency of 15 Hz, the filtered velocities were then numerically integrated and passed through the same filter, the temporal mean was also subtracted before each integration such that the accelerations, velocities, and displacements were zero mean. Considering the same stopping criteria values  $\varepsilon_1 = \varepsilon_2 = 10^{-6}$ , model selection is carried out using FRNLO+BRNLO and ESNLO algorithms. From Fig. 11, it can be seen that one more nonlinear term ( $q^7$ ) is added to the selected model when comparing with the results from Fig. 7 which is based on the response data generated from simulation. Some error introduced to the model due to the selected model with extra terms, however, the model is still reliable which is clear from Fig. 12a. By relaxing the stopping criteria one can deliver more parsimonious model with enough accuracy which discussed in Section 5 when discussing results using experimental data.

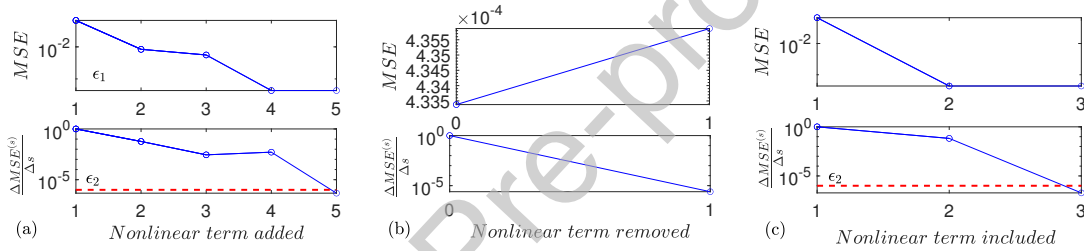


Figure 11: Nonlinear model selection for case 2 based on the data obtained from integration of acceleration (a) FRNLO (selected models:  $[|q|q^3, q^7, |q|q, q^3, |q|q^3]$ ) (b) BRNLO (selected models:  $[|q|q^3, q^7, |q|q, q^3, |q|q^5]$ ) and (c) exhaustive search (selected models:  $[|q|q, q^3, q^7]$ ) algorithms.

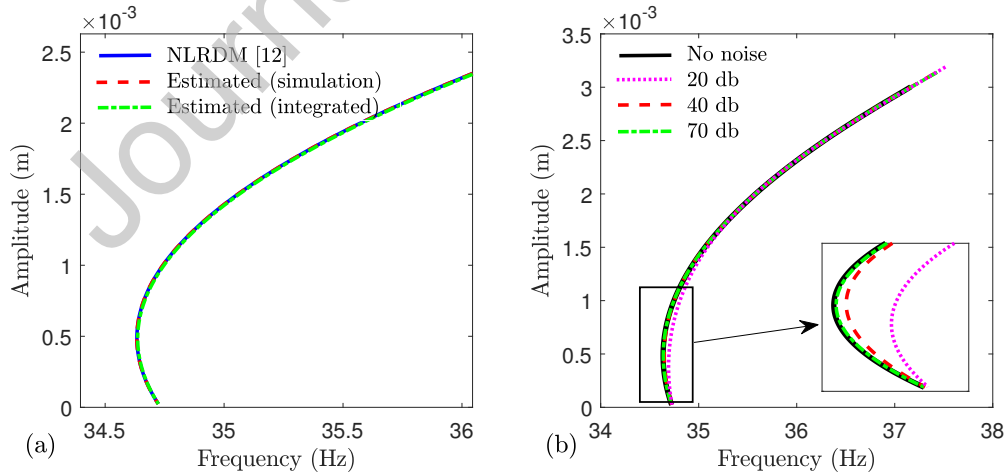


Figure 12: Comparison of backbone curve for (a) Simulation data and the data obtained from integration of acceleration (b) Different noise levels (20, 40, 70 dB).

The effects of noise level present in experimental measurement are now discussed on the model selection and parameter estimation. To simulate the test condition, similarly, Case 2 in Table 2 is evaluated by adding white Gaussian noise to the synthesised acceleration measurements considering signal-to-noise ratios (SNR) of 20, 40 and 70 dB. In practice, electromagnetic shakers typically yield a SNR of 60~80 dB, which is coherent with a noise-free assumption [38]. Therefore, the input force is assumed to be noiseless. The noise is considered on the acceleration record data and then velocity and displacement derived using integration. Fig. 12b present the backbone curves generated for data with different levels of added noise. It is observed that only high level of noise (20 db) cause some distortion in the estimated backbone curve which is evident when predicting the dynamics response at the low vibration amplitudes. Similarly, the effect of noise level on model selection is noticeable for high level of noise (20 db) as more polynomial terms are selected ( $|q|q^3, q^7, |q|q, q^3, |q|q^5, q^5$ ) when identifying the nonlinear model at the system. For medium to low level of noise, the selected model are the same to the noise free case.

The importance of including enough nonlinear models in the library of nonlinear terms is studied now. We tried to identified the system studied above in the Case 6 (dead zone) considering only polynomial models in the library of nonlinear terms. Results are presented in Fig. 13. One can see that the nonlinearity can be approximated using polynomial functions by adding the terms  $|q|q, q^3, |q|q^3, q^5, |q|q^5$ . This estimation seems to be valid for a certain range of amplitudes (higher) of the system response. However, the estimation shows important discrepancies at low amplitudes of vibration. The response of system in time-domain is presented in Fig. 13b which generally shows good agreement in terms of frequency and overall amplitude. One can see that a unique nonlinear behaviour might be described using different nonlinear models as long as that model captures important nonlinear features of the system. Furthermore, it should be noted that even simpler combination of models which satisfies the stopping criteria would be acceptable depending on the desired prediction accuracy and safety requirement.

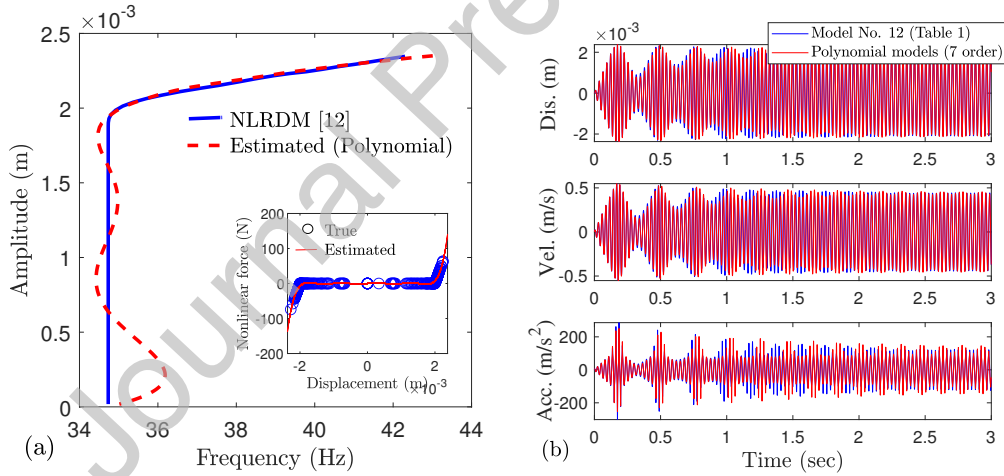


Figure 13: Comparison of fitting results to the dead zone nonlinearity using polynomial nonlinear terms only (a) Backbone curves and nonlinear force-displacement response (b) Displacement, velocity and acceleration response.

Finally, the effects of inaccurate parameters of underlying linear system are investigated considering the example Case 2 in Table 2. Approach (II) is used to formulate the cost function while FRNLO+BRNLO algorithms are used for model selection and parameter estimation. Fig. 14 shows the results of a sensitivity analysis based on 500 samples randomly generated for the pair of natural frequency and damping ratio. Normal distribution with a mean of 34.73 Hz and a standard deviation of 0.17 Hz is considered to model natural frequency variation. Generalized extreme value distribution with location parameter  $\mu = 0.0091$ , scale parameter  $\sigma = 0.0073$ , and shape parameter  $k = 0.066$  is considered for the damping ration. Extreme value distribution is used to avoid generating negative damping ratio values while allowing for a higher



375 dispersion in the randomly generated damping ratios. It can be seen in Fig. 14a that the estimated natural  
 frequency and damping ratio converge towards the true values of the linear parameters that are presented in  
 Section 3. This shows that small inaccuracies in the linear parameters can be corrected using the approach  
 (II) if the initial linear parameters are located in the basin of attraction of optimisation problem, that  
 is, if the initial linear parameters are relatively close to the true frequency and damping ratio. Fig. 14b  
 380 shows that the variation of the estimated linear parameters is low. We also notice that the model selection  
 was successful for all of the randomly generated inaccurate frequencies and damping ratios for which the  
 quadratic and cubic terms were correctly selected. Fig. 14c presents the scatter of estimated nonlinear  
 parameters versus true values which also indicates satisfactory estimation.

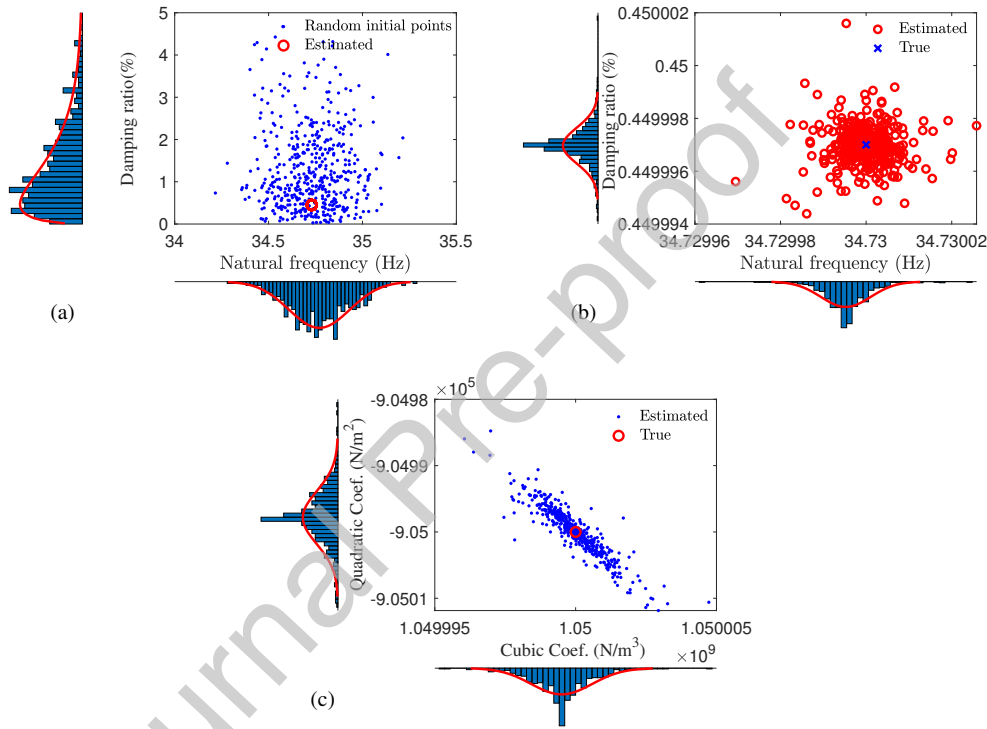


Figure 14: Effects of inaccurate underlying linear system parameters for case 2 example (a) scatter of random initial points and estimated values for natural frequency and damping ratio (b) scatter of estimated natural frequency and damping ratio versus true values (c) scatter of estimated versus true nonlinear parameters.

#### 4. Application to nonlinear MDOF systems

385 The aim of this section is to present how the framework introduced above can be extended to identify  
 nonlinear MDOF systems. The nonlinearity effect can produce cross-coupling between linear modes of  
 vibration [21, 39] in MDOF systems. The example model studied here is taken from [40] which consists of  
 two masses and one nonlinear element as shown in Fig. 15. The location of nonlinear element is defined by  
 $\rho = [1 \ 0]$ . The underlying linear system parameters and excitation force is defined as follow:

$$\mathbf{M} = \begin{bmatrix} 1 & 0 \\ 0 & 1 \end{bmatrix} \text{kg}, \mathbf{C} = \begin{bmatrix} 9.33 & 1.41 \\ 1.41 & 9.33 \end{bmatrix} \text{N.sec/m}, \mathbf{K} = \begin{bmatrix} 35619 & -3553 \\ -3553 & 35619 \end{bmatrix} \text{N/m}, \begin{bmatrix} F_1 \\ F_2 \end{bmatrix} = \begin{bmatrix} F_0 \sin(\omega t) \\ 0 \end{bmatrix} \text{N} \quad (7)$$

The linear natural frequencies are 28.5 and 31.5 Hz and mass normalized mode shapes are  $[-0.7071 \ -0.7071]^T$  and  $[-0.7071 \ 0.7071]^T$ . We rewrite the modal equations based on Eq. (2) for quadratic+cubic stiffness nonlinearity for demonstration only.

$$\begin{aligned} \ddot{\mathbf{u}}_1 + 2\zeta_1\omega_1\dot{\mathbf{u}}_1 + \omega_{m_1}^2\mathbf{u}_1 + ap(1)(a\mathbf{u}_1 + b\mathbf{u}_2)|(a\mathbf{u}_1 + b\mathbf{u}_2)| + ap(2)(a\mathbf{u}_1 + b\mathbf{u}_2)^3 &= \Phi_1^T \mathbf{F} \\ \ddot{\mathbf{u}}_2 + 2\zeta_2\omega_2\dot{\mathbf{u}}_2 + \omega_{m_2}^2\mathbf{u}_2 + bp(1)(a\mathbf{u}_1 + b\mathbf{u}_2)|(a\mathbf{u}_1 + b\mathbf{u}_2)| + bp(2)(a\mathbf{u}_1 + b\mathbf{u}_2)^3 &= \Phi_2^T \mathbf{F} \end{aligned} \quad (8)$$

Here,  $\omega_k$  is the  $k^{th}$  natural frequency of the underlying linear system and  $\zeta_k$  is the damping ratio. The nonlinearity location vector  $\rho$  and linear mode shapes  $\Phi$  are assumed to be known. In Eq. (8),  $[a, b] = \Phi^T \rho_i^T$  and, the  $j^{th}$  coefficient of the nonlinear function contributing to the system response is presented by  $p(j)$ . As it can be seen, by writing the equations of motions in terms of the linear modal coordinates, it is possible to decouple them in the linear part (assuming proportional damping) but the modal coupling created by the nonlinearities becomes evident.

For the model selection, the optimisation problem is tuned to consider one of the modal equations as the only contributor to the cost function to be optimised, while the other modal equations are considered as nonlinear inequality constraint functions according to Eq. (4). Consequently, the effect of nonlinearities in the system is considered in all of the modes at the same time and the estimated parameters will be unique. The criterion for selecting the main mode is driven by the nonlinear effect that requires to be modelled and the frequency range at which the structure must be excited to activate it.

For instance, if the structure has a nonlinearity that distorts more significantly the first resonance peak, then that mode should be targeted and the structure should be excited nearby the first linear frequency. Using the resulting response data, the first modal equation should be considered as the only contributor to the cost function, while the others will be used as constraint function.

As it was mention before, the optimisation problem can be setup for model selection and parameter estimation considering the modal equation at the excited mode as main function and the equations of other mode as constraints. Transient response of the structure when it is harmonically excited near a resonance condition for a duration of  $T=3$  sec is used for the nonlinear identification. As before, the time-domain data obtained from acceleration outputs are processed to obtain the velocity and displacement responses and provided as an input to FRNLO+BRNLO algorithms for model selection and parameters estimation. Approach I is used and the nonlinear element considered in this example (located between mass 1 and ground) is assumed to be a quadratic+cubic+quintic function with the coefficients  $-9.05 \times 10^5 \text{ N/m}^2$ ,  $1.05 \times 10^9 \text{ N/m}^3$ ,  $-3.1 \times 10^{13} \text{ N/m}^5$  respectively. Fig. 16 presents the convergence of model selection process along the forced response of mass 1 for different levels of harmonic excitation  $\mathbf{F}_0 = [2, 5, 7, 10]\text{N}$ . According to Fig. 16a,b the model selection using FRNLO results in four polynomial terms. It follows that BRNLO eliminate one term from the selected bin.

The estimated and simulated forced responses in Fig. 16c indicates a successful and accurate identification of MDOF case.

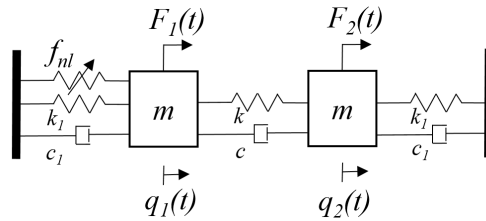


Figure 15: Two degree of freedom system with stiffness nonlinearity.

It is worth mentioning that various nonlinearities would probably trigger different internal resonances when the system excited by high level input force. Therefore, it is important that the selected nonlinear model captures these features especially in the MDOF systems. However, studying these internal resonances are beyond the scope of the present study.

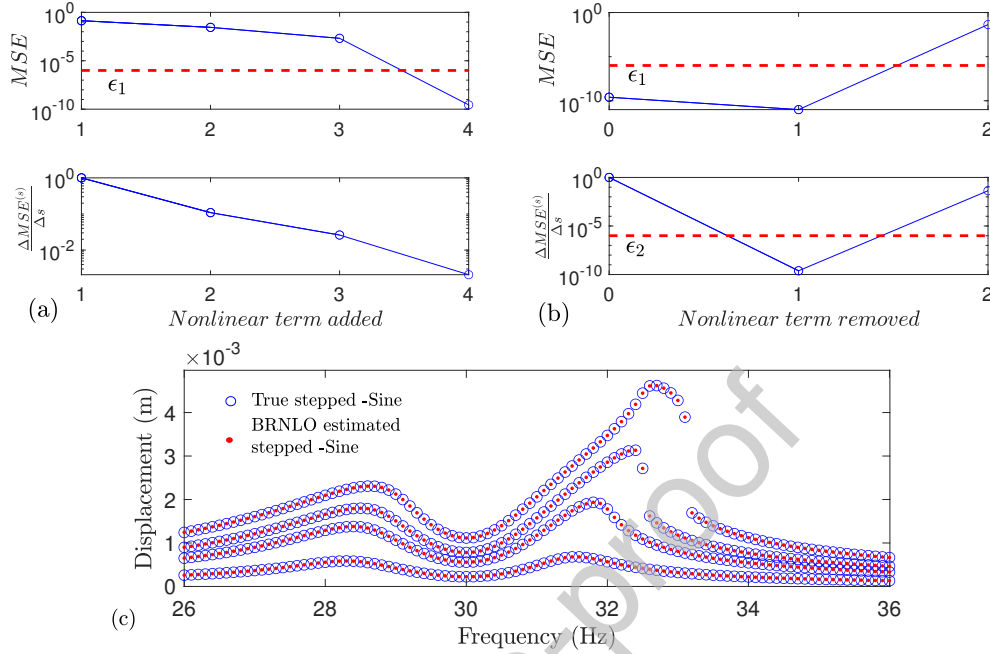


Figure 16: Identification results for 2DOF example using the FRNLO+BRNLO algorithms (a) FRNLO convergence  $[q^5, q^7, |q|q, q^5]$  (b) BRNLO convergence  $[q^3, |q|q, q^3]$  (c) forced responses of mass 1 for force levels  $\mathbf{F}_0 = [2, 5, 7, 10]$ N.

## 5. Experimental Example

The SDOF test structure considered in this work consists of a lumped mass excited on the horizontal direction and fixed to the ground with two steel plate at each side as shown in Fig. 17. The thin plates are considered as a source of geometric nonlinearity. The mass are connected to the plates using bolted joints with uniform bolt torque of 4 N.m. Friction and the uneven contact area in the joints at higher vibration amplitudes can also be regarded as another source of nonlinearity for the lightweight structure in this study. The model is excited by an electrodynamic shaker (LDSV201) and instrumented with a piezoelectric accelerometers (PCB M353B18) and one force sensor (PCB 208C02) to measure the shakers driving force. Following the measurement, the accelerations were numerically integrated, and the resulting velocity were passed through a first order high-pass Butterworth filter with a cutoff frequency of 15 Hz, the filtered velocities were then numerically integrated and passed through the same filter, the temporal mean was also subtracted before each integration such that the accelerations, velocities, and displacements were zero mean. Additionally, a laser displacement sensor (ZX2-LDA11) is used to measure the mass displacement in the horizontal direction. Laser readings are used only to verify that the displacement obtained numerically from the acceleration record is reliable. The vibration tests were controlled and recorded using Quattro Data Physics Analyser.

A single-degree-of-freedom (SDOF) model is use to model the test rig, and therefore the geometric nonlinearity is considered lumped in the degree of freedom we are using to describe the dynamic response. The results from linear modal testing using low vibration levels gives the natural frequency and damping ratio  $f_n = 34.8$  Hz,  $\zeta = 0.0045$  respectively. The identification process carried out based on approach (III). The linear parameters from linear modal testing are used to constrain the optimisation algorithm and provided the initial condition to start the optimisation with.

The model selection and parameters estimation carried out using forced response under harmonic loading with amplitude 1N and loading frequency equal to natural frequency. Free decay response by releasing the

system from a 3.3 mm initial displacement is used to validate the estimated model. The results of model selection and parameter estimation are shown in Fig. 18. The results plotted in left hand panel shows that the model selection based on FRNLO algorithm converges after adding 5 polynomial nonlinear terms ( $p(1)|q|q^3, p(2)q^7, p(3)|q|q, p(4)q^3, p(5)|q|q^5$ ) to the equation of motion where  $p(j)$  is the parameter of  $j^{th}$  nonlinear term. The  $MSE$  curve flattens and the difference between consecutive  $MSE$  drops to lower than  $\Delta MSE^{(s)}/\Delta s < \varepsilon_2$  which have been selected  $10^{-6}$ . Relaxing the stopping criteria to  $10^{-3}$  results in more parsimonious selected model ( $p(1)|q|q^3, p(2)q^7, p(3)|q|q, p(4)q^3$ ), however, it may be at the cost of a reduced prediction accuracy. FRNLO+BRNLO provides the same nonlinear model as ESNLO algorithm. To validate the selected model, stepped sine simulation results are also plotted in top of the backbone curves. In addition, the force displacement responses of nonlinear identified model are compared with the measured data which exhibits satisfactory agreement.

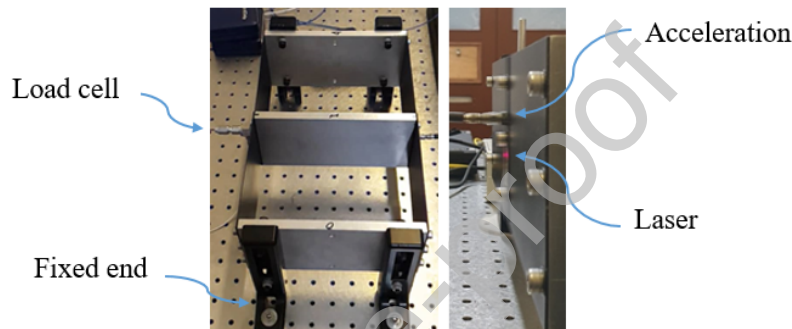


Figure 17: Experimental rig of a SDOF system with lumped mass and connecting thin steel plates.

Table 7 reports the parameter estimation results for experimental example. Adopting the selected model and estimated parameters, Fig. 18b presents the comparison between nonlinear force-displacement curves from experimental data and identified model. Also, backbone curves estimated from two identified models when setting two different stopping criteria thresholds and the experimentally measured backbone curve using NLRDM method [12] are presented. Stepped sine test responses are overlaid for different levels of excitation ( $\mathbf{F}_0 = [0.125, 0.25, 0.5, 1]N$ ). A satisfactory agreement can be observed in the results for large to low range of displacement which confirms successful identification of nonlinear dynamics of the structure in the considered domain of performance.

Fig. 19 presents the free decay response of the experimental example which is used for validation. Fig. 19a shows that the fitted model is able to predict the dynamic response of the structure. An estimation of the nonlinear force time series is presented in Fig. 19b which shows a good match between experimental and identified nonlinear forces. Results also show that the fitted model captures the nonlinear response of the structure both at lower and higher amplitudes of vibration as shown in terms of the backbone curve in Fig. 18b and in terms of the time series in Fig. 19b.

Table 7: Parameter estimation of identified model for experimental SDOF example using FRNLO+BRNLO algorithms for stopping criteria  $\varepsilon_1 = \varepsilon_2 = 10^{-6}$ .

$p(1)$ (N/m <sup>4</sup> )	$p(2)$ (N/m <sup>7</sup> )	$p(3)$ (N/m <sup>2</sup> )	$p(4)$ (N/m <sup>3</sup> )	$p(5)$ (N/m <sup>6</sup> )
$-9 \times 10^{11}$	$1.69 \times 10^{19}$	$-2.1 \times 10^6$	$2.99 \times 10^9$	$9.343 \times 10^{16}$

## 6. Conclusion

The research presents a new, data-driven method, for model selection and parameter estimation of structure containing discrete nonlinear stiffness. The structure is excited by a harmonic force near the

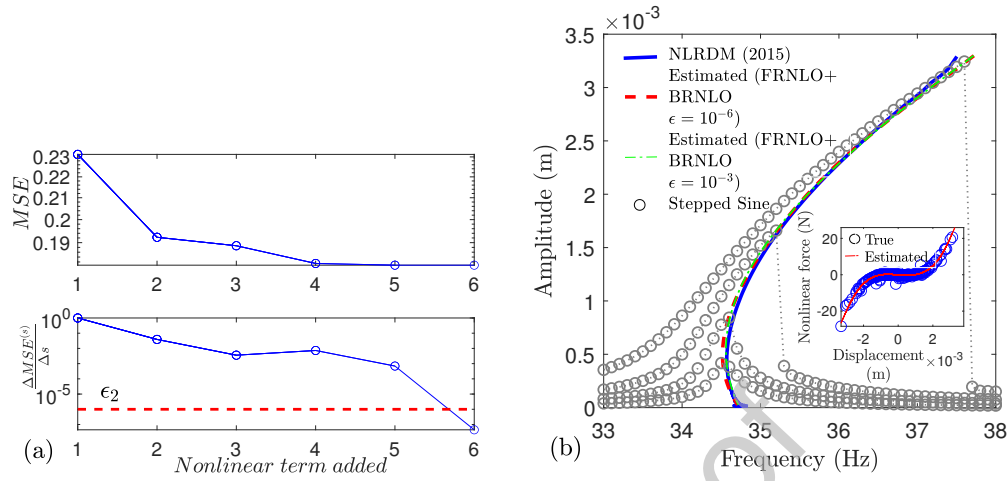


Figure 18: Identification results for experimental example using the FRNLO+BRNLO algorithms (a) Progression of model selection convergence (b) Nonlinear force-displacement and backbone curve comparison.

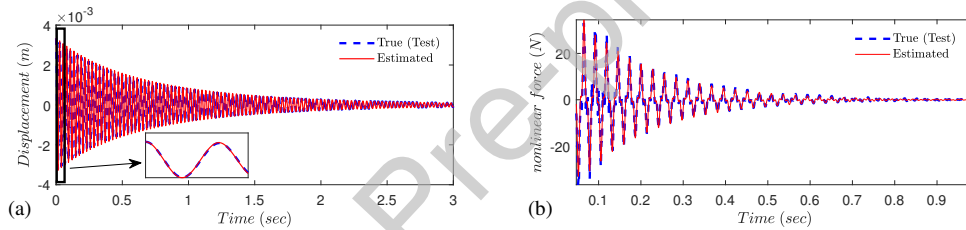


Figure 19: Comparison of time series responses of experimental example (a) Displacement of the true and identified models (b) Nonlinear force of the true and identified models.

resonance frequency of underlying linear system where the nonlinearities in the system can be activated and the transient response data recorded. This data alongside modal equations of motions that are coupled due to the presence of nonlinear terms are used to identify linear and nonlinear parameters. In the proposed method, nonlinear model selection and parameter estimation is carried out systematically at a single step using recursive optimisation-based algorithms.

Forward-backward and exhaustive search nonlinear optimisation algorithms are presented and used to select the best possible nonlinear model and estimate its parameters from a predefined library of nonlinear terms. The algorithms initiate the process using the information identified for the underlying linear system. They progress by adding nonlinear models to the equations of motions from a comprehensive predefined library of nonlinear terms. The parsimony principle is deeply embedded in the framework proposed in this paper.

Through numerical examples various nonlinear cases are investigated while considering different levels of information available from the underlying linear system. The results showed that the model selection can be carried out satisfactorily, even if no a prior knowledge about the nonlinearity is given; this provided that the library of nonlinear terms is exhaustive enough.

It was also shown that the proposed method can be extended to identifying nonlinear models for MDOF systems that have a single nonlinear element. Since there is no need to run structural simulation in each iteration, the proposed method can identify important nonlinear models efficiently. The proposed method is also demonstrated on an experimental test case study, where a nonlinear structure with geometric and bolted joint nonlinearities is examined. The presented method was capable of producing a nonlinear model

to satisfactorily describe the dynamics of the structure at low to high levels of vibration.

The framework presented in this paper is a versatile tool that can be extended to cover different kind of nonlinearities. The proposed method can be used to identify more complex nonlinear structures for which it is recommended to excite the structure in the mode which involve most important nonlinear dynamics for the expected performance level.

From a practical point of view, FRNIO+BRNLO algorithm is efficient in terms of computational time and accuracy especially when the number of nonlinear elements increases, whereas, ESNLO can be more applicable for structures with limited nonlinear elements as it generates a bulk of combinations depending on the population of predefined library of nonlinear models. The algorithms can be vastly speed up by implementing the routines in such a way that take advantage of multi-core processors and parallel computing.

Furthermore, others forms of excitation could be used for model selection and parameter estimation using the method proposed in this paper. For instance, sweep sine type excitation around the resonance frequency of interest can be used as an alternative loading instead of sine excitation. It should be noted that other types of forcing such as random excitation could be considered if the structural response amplitude is enough as to produce a strong nonlinear structural response. It is also noteworthy that the identified nonlinear model will be valid only over the amplitude range cover by the response data used in the identification task. Future works would need to assess the application of the proposed method for systems with non-proportional and nonlinear damping as they will introduce further cross couplings in the modal equations of motions. Moreover, the effects that uncertainties in the underlying linear model of nonlinear MDOF systems could have on the effectivity of nonlinear identification method presented in this paper remain unclear and need further investigation. This will help developing more robust model selection strategies for the structural systems with multiple nonlinear elements in which the effects of higher mode truncation can be addressed.

## 7. Acknowledgements

Mr Safari is support by the scholarship from the College of Engineering, Mathematics, and Physical Sciences, University of Exeter which is gratefully acknowledged.

## References

- [1] D. J. Ewins, *Modal testing: Theory, Practice, and Application.*, Engineering Dynamics Series, 2000.
- [2] J. P. Noël, G. Kerschen, Nonlinear system identification in structural dynamics: 10 more years of progress, *Mechanical Systems and Signal Processing* 83 (2017) 2–35. doi:10.1016/j.ymssp.2016.07.020.
- [3] A. D. Carri, D. J. Ewins, A systematic approach to modal testing of nonlinear structures, R. Allemang, J. De Clerck, C. Niezrecki, A. Wicks (Eds.), *Topics in Modal Analysis Conference Proceedings of the Society for Experimental Mechanics Series* 7 (2014) 273–286. doi:10.1007/978-1-4614-6585-0\_25.
- [4] D. J. Ewins, B. Weekes, A. D. Carri, Modal testing for model validation of structures with discrete nonlinearities, *Phil. Trans. R. Soc. A* 383 (2051) (2015). doi:10.1098/rsta.2014.0410.
- [5] J. R. Wright, J. E. Cooper, M. J. Desforhes, Normal mode force appropriation: Theory and application, *Mechanical Systems and Signal Processing* 13 (2) (1999) 217–240. doi:10.1006/mssp.1998.1214.
- [6] J. G. Kerschen, J. C. Golinval, K. Worden, Theoretical and experimental identification of a non-linear beam, *Journal of Sound and Vibration* 244 (4) (2001) 597–613. doi:10.1006/jsvi.2000.3490.
- [7] C. M. Richards, R. Singh, Identification of multi-degree-of-freedom non-linear systems under random excitation by the “reverse path” spectral method, *Journal of Sound and Vibration* 213 (4) (1998) 673–708. doi:10.1016/j.ymssp.2017.06.017.
- [8] P. Muhamad, N. D. Sims, K. Worden, On the orthogonalised reverse path method for nonlinear system identification, *Journal of Sound and Vibration* 331 (20) (2012) 4488–4503. doi:10.1016/j.jsv.2012.04.034.
- [9] S. Marchesiello, L. Garibaldi, A time domain approach for identifying nonlinear vibrating structures by subspace methods, *Mechanical Systems and Signal Processing* 22 (1) (2008) 81–101. doi:10.1016/j.ymssp.2013.10.016.
- [10] J. P. Noël, S. Marchesiello, G. Kerschen, Subspace-based identification of a nonlinear spacecraft in the time and frequency domains, *Mechanical Systems and Signal Processing* 43 (2014) 217–236. doi:10.1016/j.ymssp.2013.10.016.
- [11] S. A. Billings, *Nonlinear System Identification: NARMAX Methods in the Time, Frequency and Spatio-Temporal Domains*, Wiley, 2013.
- [12] J. M. Londoño, S. Neild, J. E. Cooper, Identification of backbone curves of nonlinear systems from resonance decay responses, *Journal of Sound and Vibration* 348 (2015) 224–238. doi:10.1016/j.jsv.2015.03.015.
- [13] J. M. Londoño, J. E. Cooper, S. Neild, Identification of systems containing nonlinear stiffnesses using backbone curves, *Mechanical Systems and Signal Processing* 84 (B) (2017) 116–135. doi:10.1016/j.ymssp.2016.02.008.

- [14] T. Hill, P. Green, A. Cammarano, S. Neild, Fast bayesian identification of a class of elastic weakly nonlinear systems using backbone curves, *Journal of Sound and Vibration* 360 (2016) 156–170. doi:10.1016/j.jsv.2015.09.007.
- [15] K. J. Moore, Characteristic nonlinear system identification: A data-driven approach for local nonlinear attachments, *Mechanical Systems and Signal Processing* 131 (2019) 335–347. doi:10.1016/j.ymssp.2019.05.066.
- [16] C. Ligeikis, A. Bouma, J. Shim, S. Manzato, R. Kuether, D. Roettgen, Modeling and experimental validation of a pylon subassembly mockup with multiple nonlinearities, in: G. Kerschen, M. Brake, L. Renson (Eds.), *Nonlinear Structures and Systems*, Vol. 1 of 38, 2020.
- [17] D. Barton, B. Mann, S. Burrow, Control-based continuation for investigating nonlinear experiments, *Journal of Vibration and Control* 18 (4) (2012) 509–520. doi:10.1177/1077546310384004.
- [18] L. Renson, A. Gonzalez-Buelga, D. Barton, S. Neild, Robust identification of backbone curves using control-based continuation, *Journal of Sound and Vibration* 367 (2016) 145–158. doi:10.1016/j.jsv.2015.12.035.
- [19] V. Denis, M. Jossic, C. Giraud-Audine, B. Chomette, A. Renault, O. Thomas, Identification of nonlinear modes using phase-locked-loop experimental continuation and normal form, *Mechanical Systems and Signal Processing* 106 (2018) 430–452. doi:10.1016/j.ymssp.2018.01.014.
- [20] M. Volvert, G. Kerschen, Phase resonance nonlinear modes of mechanical systems (2020). arXiv:2010.14892.
- [21] L. Renson, T. L. Hill, D. A. Ehrhardt, D. A. W. Barton, S. A. Neild, Force appropriation of nonlinear structures, *Proc. R. Soc. A* 474 (2214) (2018). doi:10.1098/rspa.2017.0880.
- [22] A. D. Carri, B. Weekes, D. DiMaio, D. J. Ewins, Extending modal testing technology for model validation of engineering structures with sparse nonlinearities: A first case study, *Mechanical Systems and Signal Processing* 84 (B) (2017) 97–115. doi:10.1016/j.ymssp.2016.04.012.
- [23] S. B. Cooper, D. DiMaio, D. J. Ewins, Integration of system identification and finite element modelling of nonlinear vibrating structures, *Mechanical Systems and Signal Processing* 102 (2018) 401–430. doi:10.1016/j.ymssp.2017.09.031.
- [24] J. Paduart, L. Lauwers, J. Swevers, K. Smolders, J. Schoukens, R. Pintelon, Identification of nonlinear systems using polynomial nonlinear state space models, *Automatica* 46 (4) (2010) 647–657. doi:10.1016/j.automatica.2010.01.001.
- [25] D. T. Westwick, G. Hollander, K. Karami, J. Schoukens, Using decoupling methods to reduce polynomial narx models, *IFAC-PapersOnLine* 51 (15) (2018) 796–801. doi:10.1016/j.ifacol.2018.09.133.
- [26] M. Platten, J. Wright, K. Worden, G. Dimitriadis, J. Cooper, Non-linear identification in modal space using a genetic algorithm approach for model selection, *International Journal of Applied Mathematics and Mechanics* 3 (1) (2007) 72–89.
- [27] P. Gluzmann, D. Panigo, Global search regression: A new automatic model-selection technique for cross-section, time-series, and panel-data regressions, *The Stata Journal* 15 (2) (2015) 325–349. doi:10.1177/1536867X1501500201.
- [28] A. B. Abdessalem, N. Dervilis, D. Wagg, K. Worden, Model selection and parameter estimation in structural dynamics using approximate bayesian computation, *Mechanical Systems and Signal Processing* 99 (2018) 306–325. doi:10.1016/j.ymssp.2017.06.017.
- [29] J. Taghipour, H. H. Khodaparast, M. I. Friswell, H. Jalali, An optimization-based framework for nonlinear model selection and identification, *Vibration* 2 (2019) 311–331. doi:10.3390/vibration2040020.
- [30] P. Peeters, H. Auweraera, P. Guillaume, J. Leuridan, The polymax frequency-domain method: a new standard for modal parameter estimation?, *Shock and Vibration* 11 (2004) 395–409. doi:10.1155/2004/523692.
- [31] K. J. Moore, M. Kurt, M. Eriten, M. D. McFarland, L. A. Bergman, A. F. Vakakis, Direct detection of nonlinear modal interactions from time series measurements, *Mechanical Systems and Signal Processing* 125 (2019) 311–329. doi:10.1016/j.ymssp.2017.09.010.
- [32] K. J. Moore, M. Kurt, M. Eriten, M. D. McFarland, L. A. Bergman, A. F. Vakakis, Time-series-based nonlinear system identification of strongly nonlinear attachments, *Journal of Sound and Vibration* 438 (2019) 13–32. doi:10.1016/j.jsv.2018.09.033.
- [33] R. E. Kalman, A new approach to linear filtering and prediction problems, *Journal of Basic Engineering* 82 (1960) 35–45. doi:10.1115/1.3662552.
- [34] A. A. Chanerley, N. A. Alexander, J. Berrill, H. Avery, B. Halldorsson, R. Sigbjornsson, Concerning baseline errors in the form of acceleration transients when recovering displacements from strong motion records using the undecimated wavelet transform, *Bulletin of the Seismological Society of America* 103 (1) (2013) 283–295. doi:10.1785/0120110352.
- [35] A. Messac, *Optimization in Practice with MATLAB*, for Engineering Students and professionals, Cambridge University Press, 2015.
- [36] Z. Ugray, L. Lasdon, J. Plummer, F. Glover, J. Kelly, R. Martí, Scatter search and local nlp solvers: A multistart framework for global optimization, *INFORMS Journal on Computing* 19 (3) (2007) 328–340. doi:10.1287/ijoc.1060.0175.
- [37] J. Yoon, B. Kim, Effect and feasibility analysis of the smoothening functions for clearance-type nonlinearity in a practical driveline system, *Nonlinear Dynamics* 85 (2016) 1651–1664. doi:10.1007/s11071-016-2784-3.
- [38] J. P. Noël, A. F. Esfahani, G. Kerschen, J. Schoukens, A nonlinear state-space approach to hysteresis identification, *Mechanical Systems and Signal Processing* 84 (B) (2017) 171–184. doi:10.1016/j.ymssp.2016.08.025.
- [39] I. Tartaruga, A. Elliott, T. L. Hill, S. A. Neild, A. Cammarano, The effect of nonlinear cross-coupling on reduced-order modelling, *International Journal of Non-Linear Mechanics* 116 (2019) 7–17. doi:10.1016/j.ijnonlinmec.2019.05.006.
- [40] M. A. Al-Hadid, J. R. Wright, Developments in the force-state mapping technique for non-linear systems and the extension to the location of nonlinear elements in the lumped-parameter system, *Mechanical Systems and Signal Processing* 3 (3) (1989) 269–290. doi:10.1016/0888-3270(89)90053-8.

Sina Safari: Conceptualization; Investigation; Methodology; Software; Validation; Visualization;  
Writing - original draft; Writing - review & editing

Julián M. Londoño Monsalve: Conceptualization; Investigation; Methodology; Software; Supervision;  
Validation; Visualization; Writing - review & editing

Journal Pre-proof



\*Declaration of Interest Statement

**Declaration of interests**

The authors declare that they have no known competing financial interests or personal relationships that could have appeared to influence the work reported in this paper.

The authors declare the following financial interests/personal relationships which may be considered as potential competing interests:

Journal Pre-proof